Aalborg Universitet

AALBORG UNIVERSITY

DENMARK

Low-Voltage Consumption Coordination for Loss Minimization and Voltage Control

Juelsgaard, Morten; Sloth, Christoffer; Wisniewski, Rafal

Low-Voltage Consumption Coordination for Loss Minimization and Voltage Control

Morten Juelsgaard, Christoffer Sloth, and Rafael Wisniewski

Section of Automation and Control, University of Aalborg,

Email: {MJU, CES, RAF}@ES.AAU.DK

Abstract— This work presents a strategy for minimizing active power losses in low-voltage grids, by coordinating the consumption of electric vehicles and power generation from solar panels. We show that minimizing losses, also reduces voltage variations, and illustrate how this may be employed for increasing the number of electric vehicles and photovoltaic systems in the grid without violating grid constraints.

I. INTRODUCTION

It is a political and scientific goal of Denmark that the entire energy supply should be based on renewable resources by 2050 [1]. For electricity production, this means that traditional fossil fired power plants must be decommissioned, and replaced with renewable alternatives, such as wind and solar. Increased use of these resources carries a transformation of the traditional electrical grid, with few centralized power plants, into a far more distributed grid, with a significant level of distributed and local power production. Introducing local power production entails bidirectional power flow between the high-voltage and low-voltage grids.

Reducing the use of fossil fuels for transportation requires an increased use of, *e.g.*, electric vehicles (EVs), and the use of these are thereby expected to increase [2], [3]. However, the current lack of charging rules or guidelines, entail that the low-voltage distribution grid is currently not suited for large scale implementation of EVs, due to the risk of grid-overload and unacceptable voltage drops [4].

Traditional measures for maintaining stable voltages in low-voltage (LV) grids, are based on an assumption of uni-directional power flow, such that the voltage will drop along the feeder. As bi-directional power flows become increasingly common, this will not pertain to be the case, requiring revisions of the traditional control strategies [5].

In [6], it was illustrated how minimization of active losses in the LV grid, could cause the voltage variations to be limited, even when many EVs where charged. In this work, we expand on this idea, and show how loss minimization can be used for coordinating consumption by EVs against production from solar panels, in order to increase the possible installation of both, without unacceptable voltage variations.

Active control of consumers, with the purpose of avoiding voltage variations and grid overload has been considered by *e.g.*, [4], [7], however these works considered only introduction of EVs and photo-voltaics (PVs) separately, and not a combination of the two. Also, the approaches of these works, were based on heuristics and a 'rule-of-thumb'

based strategies, whereas our work employs an underlaying optimization for coordination.

Loss minimization was the main focus of [8], who considered grid reconfiguration for loss reduction, and [9], [10], who considered how and where to locate distributed generation, such as PVs, in the LV grid, in order to reduce losses. Compared to these works, this paper does not attempt to modify the grid or pick beneficial PV installation locations. Rather, we will outline a coordination strategy which can be employed for loss reduction following a chosen installation of PVs.

The remaining paper is organized as follows: Section II outlines our modeling approach, and presents the formal problem description. Section III addresses our approach towards solving the coordination problem, and describes a benchmark strategy for result comparison. A practical test-case, used for numerical experiments, is presented in Section IV, followed by examples in Section V. Concluding remarks are presented in Section VI.

II. MODELING AND PROBLEM FORMULATION

In this section, the considered low-voltage grid is modeled, and the optimization problem for minimizing active power losses is set up.

The grid consists of households with flexible reactive power production from PVs, and flexible power consumption from EVs. In addition, each household has an inflexible consumption that is an aggregation of all types of consumption that does not allow temporal shifts, such as lighting, cooking, and television. We study the problem of minimizing active power losses, while satisfying voltage constraints.

The low-voltage (0.4 kV) grid consists of residential households interconnected by transmission lines in a tree topology. The LV grid is connected to the medium voltage grid, through a transformer. This is illustrated in Fig. 1.

For simplicity, the medium voltage grid and transformer station are abstracted by an ideal voltage supply, i.e., the secondary side root-mean-square (RMS) voltage of the transformer $u_s \in \mathbf{R}$, has a constant magnitude and frequency. In addition, we assume that the grid is balanced. This allows the analysis of an equivalent single phase system [11]. Throughout, we consider only average active and reactive power over some time period; not instantaneous power.

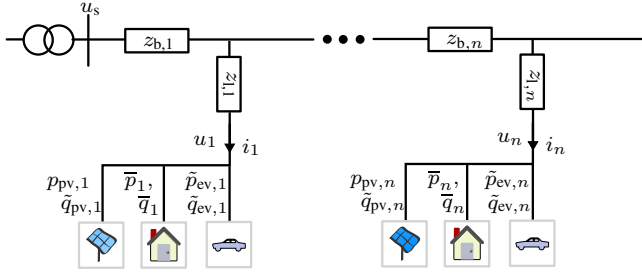The transmission lines are modeled as approximate π-circuit models, where the shunt capacitances are neglected,

Fig. 1. Conceptual outline of a radial of the low-voltage grid, illustrating the consumers, with active and reactive solar production $(p_{\text{pv},i}, q_{\text{pv},i})$, EV consumption $(p_{\text{ev},i}, q_{\text{ev},i})$, and inflexible consumption $(\tilde{p}_i, \tilde{q}_i)$.

since the cables in the considered grid are short. Thus, transmission lines are modeled as RL-series impedances.

The grid consists of two different types of transmission lines: branch lines and leaf lines. Along the radial, there are branch lines with impedance $z_{\text{b}} \in \mathbf{C}$, which we refer to as branch-impedances. Similarly, each household is connected to the radial through a leaf line, with leaf impedance $z_{\text{l}} \in \mathbf{C}$. The impedances of branch h and leaf k are

$$z_{\text{b},h} = r_{\text{b},h} + \mathrm{j}\omega L_{\text{b},h}, \quad \text{and} \quad z_{\text{l},k} = r_{\text{l},k} + \mathrm{j}\omega L_{\text{l},k},$$

with ω denoting the grid frequency.

The n households in the grid are modeled as potential prosumers (producers and consumers), with power consumption for every household $h \in H \equiv \{1, \dots, n\}$, given by

$$p_h = \overline{p}_h + \tilde{p}_h, \quad \text{and} \quad q_h = \overline{q}_h + \tilde{q}_h,$$

where $\overline{p}_h$ and $\overline{q}_h$ are the inflexible active respectively reactive power consumption, and $\tilde{p}_h$ and $\tilde{q}_h$ are the flexible active respectively reactive power consumption.

The subset $H_{\text{ev}} \subseteq H$, denotes households with EVs, providing flexible consumption at a constant power factor ψ_h. We consider a time-frame $\mathcal{T}$ divided into m periods of duration T_{s}, i.e.

$$\mathcal{T} \equiv \{1, \dots, m\}.$$

The flexible consumption from each EV is constrained in the sense that for all $h \in H_{\text{ev}}$

$$\sum_{t=t_{\text{ev},h}}^{m} T_{\text{s}} \tilde{p}_{\text{ev},h}(t) + E_{\text{ev},h}(t_{\text{ev},h}) = E_{\text{dem},h},$$

$$E_{\min,h} \leq \sum_{t=t_{\text{ev},h}}^{\tau} T_{\text{s}} \tilde{p}_{\text{ev},h}(t) + E_{\text{ev},h}(t_{\text{ev},h}) \leq E_{\max,h},$$

$$p_{\min,h} \leq \tilde{p}_{\text{ev},h}(t) \leq p_{\max,h},$$
$$\tilde{q}_{\text{ev},h}(t) = \tilde{p}_{\text{ev},h}(t) \tan(\text{acos}(\psi_h)),$$

for all $\tau, t \in \mathcal{T}$, where $\tilde{p}_{\text{ev},h}(t)$ and $\tilde{q}_{\text{ev},h}(t)$ are active and reactive power consumed by the EV in time period t, $E_{\text{ev},h}(t_{\text{ev},h})$ is the charge of the EV in the beginning of time period $t_{\text{ev},h}$, and $t_{\text{ev},h}$ is the time where the EV starts charging. Further, $E_{\text{dem},h}$, $E_{\min,h}$, and $E_{\max,h}$ denote required final level of charge, and lower and upper charge limits of the EV battery. Similarly, $p_{\min,h}$ and $p_{\max,h}$ are minimum and maximum power limits for each EV battery. For $h \notin H_{\text{ev}}$, $\tilde{p}_{\text{ev},h}(t), \tilde{q}_{\text{ev},h}(t) \equiv 0$ for all $t \in \mathcal{T}$.

The subset $H_{\text{pv}} \subseteq H$ denotes households with PV installed. These produce active power $p_{\text{pv},h}(t) \geq 0$, and reactive power $\tilde{q}_{\text{pv},h}(t)$. The active power is determined from

weather conditions, i.e. direct/indirect radiation, clouds etc. On the other hand, the reactive power is controllable, with the constraint

$$|\tilde{q}_{\text{pv},h}(t)| \leq \sqrt{s_{\max,h}^2 - p_{\text{pv},h}^2(t)}, \quad \forall t \in \mathcal{T}$$

where $s_{\max,h} > 0$ is a fixed upper limit of apparent power for the solar panel inverter. This constraint is similar to the work by [7]. For all $h \notin H_{\text{pv}}$, we define $p_{\text{pv},h}(t), \tilde{q}_{\text{pv},h}(t) \equiv 0$, for all $t \in \mathcal{T}$.

The total active and reactive power of a consumer is then

$$p_h(t) = \overline{p}_h(t) + \tilde{p}_{\text{ev},h}(t) - p_{\text{pv},h}(t),$$

$$q_h(t) = \overline{q}_h(t) + \tilde{q}_{\text{ev},h}(t) - \tilde{q}_{\text{pv},h}(t).$$

The RMS phasor-voltage in the connection point of consumer h, is denoted $u_h(t) \in \mathbf{C}$. The corresponding RMS phasor-current $i_h(t) \in \mathbf{C}$, drawn by the consumer is then

$$i_h(t) = \left(\frac{p_h(t) + \mathrm{j}q_h(t)}{u_h(t)}\right)^\dagger, \quad (1)$$

where $\dagger$ denotes conjugate transpose [12].

The current $i_h(t)$ passes through a number of branches, and one leaf, in order to reach the consumer. For a radial containing M branches, let $B_h \subset B \equiv \{1, \dots M\}$ be the index set of the branches passed by i_h, for each $h \in H$. Let

$$i(t) = (i_1(t), \dots, i_n(t)), \quad u(t) = (u_1(t), \dots, u_n(t)),$$

i.e., $i(t), u(t) \in \mathbf{C}^n$, for all t. Further, define the matrices $J_{\text{r}} \in \mathbf{R}^{n \times n}$ and $J_{\text{z}} \in \mathbf{C}^{n \times n}$ as:

$$[J_{\text{r}}]_{x,y} = \begin{cases} \sum_{h \in B_x} r_{\text{b},h} + r_{\text{l},x}, & x = y \\ \sum_{h \in (B_x \cup B_y)} r_{\text{b},h}, & x \neq y, \end{cases}$$

and

$$[J_{\text{z}}]_{x,y} = \begin{cases} \sum_{h \in B_x} z_{\text{b},h} + z_{\text{l},x}, & x = y \\ \sum_{h \in (B_x \cup B_y)} z_{\text{b},h}, & x \neq y. \end{cases}$$

It can be shown, that the total active power loss in the radial, $p_{\text{d}}(t) \in \mathbf{R}_+$, can be expressed as

$$p_{\text{d}}(t) = i(t)^\dagger J_{\text{r}} i(t) > 0,$$

and the voltage at each household can be expressed by

$$u(t) = u_{\text{s}} - J_{\text{z}} i(t),$$

for all $t \in \mathcal{T}$. Power quality demands, require that the grid is managed such that voltage variations throughout the radial are limited, i.e.,

$$u_{\min} \leq |u(t)| \leq u_{\max}, \quad \forall t \in \mathcal{T}, \quad (2)$$

where $|\cdot|$ denotes entry-wise complex magnitude, and $u_{\min}, u_{\max} \in \mathbf{R}$ are lower and upper bound on voltage magnitudes, respectively. The inequalities above are to be read element-wise.

Given the losses and constraints described above, we state the following main problem.

Problem 1: Given the topology of a radial, with branch and leaf impedances, as well as households H with flexibility $H_{ev}, H_{pv} \subseteq H$, and $\bar{p}_h(t), p_{pv,h}(t), \bar{q}_h(t), \psi_h, t_{ev,h}$, solve

$$\underset{\substack{\tilde{p}_{ev,h}(t), \tilde{q}_{pv,h}(t) \\ h \in H, t \in \mathcal{T}}}{\text{minimize}} \quad \sum_{t=1}^{m} p_d(t)$$

subject to
$$u_{\min} \leq |u(t)| \leq u_{\max},$$
$$p_{\min,h} \leq \tilde{p}_{ev,h}(t) \leq p_{\max,h},$$
$$T_s \sum_{t=t_{ev,h}}^{\tau} \tilde{p}_{ev,h}(t) \in [\delta E_{\min,h}, \ \delta E_{\max,h}], \quad (3)$$
$$T_s \sum_{t=t_{ev,h}}^{m} \tilde{p}_{ev,h}(t) = \delta E_{dem,h},$$
$$\tilde{q}_{pv,h}(t) \leq \sqrt{s_{\max,h}^2 - p_{pv,h}^2(t)},$$
$$i_h(t) = \frac{p_h(t) - jq_h(t)}{u_h^{\dagger}(t)},$$

for all $t, \tau \in \mathcal{T}$, $h \in H$, with $\delta E_{\max,h} = E_{\max,h} - E_{ev,h}(t_{ev,h})$, $\delta E_{\min,h} = E_{\min,h} - E_{ev,h}(t_{ev,h})$, and $\delta E_{dem,h} = E_{dem,h} - E_{ev,h}(t_{ev,h})$..

In the next section, we elaborate on our approach for solving Problem 1, and formulate a benchmark strategy, which we use for comparison during numerical experiments.

III. Optimization and benchmark

Our strategy is to identify the non-convex elements of Problem 1, in order to make convex approximations, and arrange a simplified problem, which we can solve globally, with known methods.

A. Optimization

Large parts of Problem 1 are convex, and requires thereby no simplifications. Recall for instance the cost function:

$$\sum_{t=1}^{m} p_d(t) = \sum_{t=1}^{m} i(t)^{\dagger} J_r i(t).$$

This cost describes the accumulated active power losses of the radial. It can be shown to be convex in the real and imaginary parts of $i(t)$, respectively. The same applies for the thermal capacity constraint. The only elements of (3) that are not convex, are the relations between $p_h(t), q_h(t)$ and $i_h(t)$ in (1), and the voltage limits (2).

The voltage constraint (2) can be visualized as the annulus in Fig. 2, where the maximum allowed amplitude is in fact convex in the real and imaginary part, respectively. The lower limit can be approximated, by the convex constraint

$$\text{Re}(u) \geq u_{\min},$$

i.e., the real part must be larger than the lower limit, as visualized by the dashed line in the figure. This approximation is commonly used [7], [13].

The consistency constraint (1), is non-convex on account of the division by $u_h^{\dagger}(t)$. We replace $u_h^{\dagger}(t)$ by a known, a priori estimate, $\hat{u}_h^{\dagger}(t)$, whereby (1) is approximated as

$$i_h(t) = \frac{p_h(t) - jq_h(t)}{\hat{u}_h^{\dagger}(t)}. \quad (4)$$

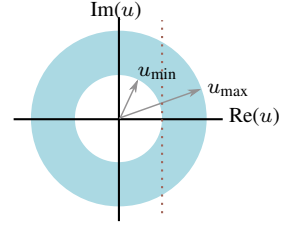Fig. 2. Constraint for the voltage amplitude, where the shaded region visualizes the allowed range of u. The dashed line illustrates the approximated constraint for the lower limit.

Given that $\hat{u}_h^{\dagger}(t)$ is a known estimate, (4) is linear. With these convexifications, the following problem can be stated as an approximation to Problem 1:

Problem 2: Provided the same information as in Problem 1, as well as a known estimate of the voltages $\hat{u}_h(t)$, for every $h \in H, t \in \mathcal{T}$, solve

$$\underset{\substack{\tilde{p}_{ev,h}(t), \tilde{q}_{pv,h}(t) \\ h \in H, t \in \mathcal{T}}}{\text{minimize}} \quad \sum_{t=1}^{m} p_d(t)$$

subject to
$$|u(t)| \leq u_{\max}, \quad \text{Re}(u(t)) \geq u_{\min}$$
$$p_{\min,h} \leq \tilde{p}_{ev,h}(t) \leq p_{\max,h},$$
$$T_s \sum_{t=t_{ev,h}}^{\tau} \tilde{p}_{ev,h}(t) \in [\delta E_{\min,h}, \ \delta E_{\max,h}], \quad (5)$$
$$T_s \sum_{t=t_{ev,h}}^{m} \tilde{p}_{ev,h}(t) = \delta E_{dem,h},$$
$$\tilde{q}_{pv,h}(t) \leq \sqrt{s_{\max,h}^2 - p_{pv,h}^2(t)},$$
$$i_h(t) = \frac{p_h(t) - jq_h(t)}{\hat{u}_h^{\dagger}(t)},$$

for all $t, \tau \in \mathcal{T}$, $h \in H$, with $\delta E_{dem,h}, \delta E_{\max,h}, \delta E_{\min,h}$ defined as in Problem 1.

Problem 2 is convex and can be solved by known methods. Let the solution be denoted $i(t)^{\star}, q(t)^{\star}, p(t)^{\star}$, with

$$p(t)^{\star} = (p_1(t)^{\star}, \cdots, p_n(t)^{\star}), \quad q(t)^{\star} = (q_1(t)^{\star}, \cdots, q_n(t)^{\star}).$$

Since (5) was solved with an estimated voltage, the true voltage may now be found through the post calculation

$$u_{\text{true}}(t) = u_s - J_z i(t)^{\star}, \quad \forall t \in \mathcal{T}.$$

Let $\hat{u}(t) = (\hat{u}_1(t), \cdots, \hat{u}_n(t))$. If

$$\|u_{\text{true}}(t) - \hat{u}(t)\| > \epsilon, \quad \forall t \in \mathcal{T},$$

for some tolerance $\epsilon > 0$, then the a priori estimate of the voltage was not sufficiently accurate. Our approach is then to update the voltage estimate, and re-solve Problem 2. This iterative approach can be formulated as in Algorithm 1.

If the iterative procedure converges such that $\|u_{\text{true}}(t) - \hat{u}(t)\| < \epsilon$, then $i^{\star}(t), q^{\star}(t), p^{\star}(t)$ are used as approximate solutions to the initial Problem 1.

B. Benchmark strategy

To illustrate the benefits of shifting the charge cycle of EVs, and utilizing reactive power control of the PVs, we present a benchmark strategy that does not utilize this

Algorithm 1: Loss minimization procedure

Initialize $\hat{u}(t) = \mathbf{1}$ pu, for all t, $\gamma = 1$, $\epsilon \in (0,\ 1)$
while $\gamma > \epsilon$ **do**

- Solve Problem 2 to obtain $i^\star(t), q^\star(t), p^\star(t)$, for each t
- Calculate true voltage:
  $u_{\text{true}}(t) = u_{\text{s}} - J_z i^\star(t), \forall t \in \mathcal{T}$
- Set $\gamma = \|u_{\text{true}}(t) - \hat{u}(t)\|$,
- Set $\hat{u}(t) = u_{\text{true}}(t)$, for all t

end

Fig. 3. Outline of the feeder employed for numerical experiments.

flexibility. That is, the benchmark strategy charges each EV, when it is plugged is. Further, the use of solar panels is limited in the sense that the capability of absorbing or producing reactive power to and from the grid, is not utilized.

The benchmark strategy thereby entails

$$\tilde{q}_{\text{pv},h}(t) = 0, \forall h \in H, t \in \mathcal{T},$$

and

$$\tilde{p}_{\text{ev},h}(t) = \begin{cases} p_{\max,h}, & \text{if } t \geq t_{\text{ev},h} \text{ and } T_s \sum_{t=t_{\text{ev},h}}^{m} \tilde{p}_{\text{ev},h}(t) < \delta E_{\text{dem},h} \\ 0, & \text{otherwise.} \end{cases}$$

The reactive power from EVs are calculated similar to previous.

The active and reactive power of each household, following the benchmark strategy, is then

$$p_h(t) = \overline{p}_h(t) + \tilde{p}_{\text{ev},h}(t) - p_{\text{pv},h}(t),$$

$$q_h(t) = \overline{q}_h(t) + \tilde{q}_{\text{ev},h}(t).$$

From the radial topology, as well as branch and leaf impedances, the radial admittance matrix Y can be arranged [11]. Given Y, as well as $p_h(t), q_h(t)$ for each $h \in H, t \in \mathcal{T}$, known methods exists for calculating the current and voltage of each consumer, e.g., Gauss-Seidel and Newton-Raphson.

The following section describes in detail a test-case used as a foundation for numerical experiments in Section V.

IV. TEST-CASE

The following test-case is to a large extend similar to a case explored by [4]. We consider a low-voltage distribution grid, of a residential neighborhood, located in Northern Jutland, Denmark. The entire low-voltage grid consists of three 10/0.4 kV transformer substations, with a total of 19 feeders and 316 residential consumers. We limit our attention to one of these feeders, servicing 34 residential consumers. The tree topology of the feeder, is illustrated in Fig. 3. As illustrated in the figure, the feeder consists of 11 branches, and 34 leafs. Each leaf represents a consumer, as illustrated with arrows. Each consumer $h \in \{1, \ldots, 34\}$ is modeled as described in Section II.

Each horizontal line, as well as all leafs, represents buses in the feeder. The initial bus labeled u_{s} represents the transformer output, modeled as a fixed voltage, slack line, cf., Section II.
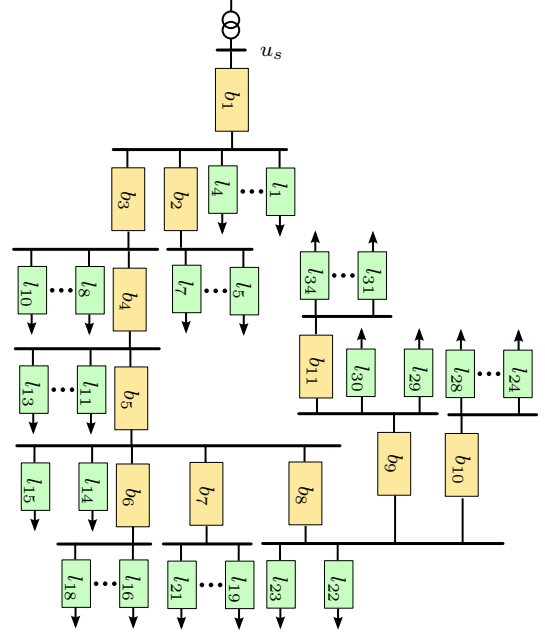
The resistive and reactive parameters of each branch and leaf, are presented in the following table. There are three different types of branches, but all leafs are characterized by the same parameters [4].

Cable type	Res. [Ω/m]	Reac. [Ω/m]
b_1, b_3, b_4	0.21	0.072
b_5, b_8	0.32	0.075
b_2, b_6, b_7, b_9-b_{11}	0.64	0.079
l_1-l_{34}	1.81	0.094

In this work, we assume a standard length of all branches of 200 m, and a standard length of each leaf of 50 m. Combined with the data above, the specific impedance of each branch and leaf can be calculated. In the numerical experiments to follow, we consider a time-period of 24 hours, starting at 14:30. The inflexible consumption of each consumer is modeled as known curves, presented in Fig. 4. The data in Fig. 4 is downloaded from Nordpool [14], and is representative of the daily consumption pattern of residential homes. With the curves in Fig. 4, the average daily energy consumption is 7.9 kWh. The inflexible consumption of all households are modeled with a constant power factor of 0.95.
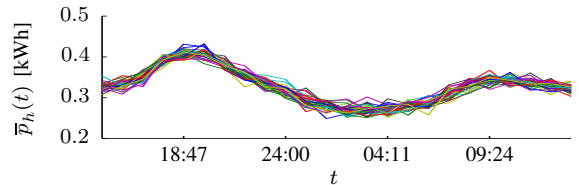

Fig. 4. The inflexible consumption of all households.

V. NUMERICAL EXPERIMENTS

In the following numerical experiments, we explore several different scenarios, related to the installation of EVs and PVs in the test-case, and illustrate how loss minimization through Problem 1, indirectly reduces voltage variations. We examine the following scenarios:

A. Resilience of benchmark strategy against implementation of EVs and PVs separately.
B. Resilience of optimization based strategy against implementation of EVs and PVs separately.
C. Benefit of optimization strategy over benchmark, with combined installations of EVs and PVs.

Scenario A shows that by separately introducing EVs and PVs, unacceptable over- and under-voltages occur, if the inherent flexibility is not utilized. Scenario B shows that the under-voltage issues of Scenario A caused by EVs can be alleviated by changing the charging profile via the proposed optimization strategy. However, the over-voltages caused by separate installation of PVs cannot be accommodated. Finally, Scenario C shows that by combining the installation of EVs and PVs, all voltage issues can be alleviated by the proposed optimization strategy.

We employ pr-unit measures in all experiments, where we choose the base voltage, $u_{\text{base}} = 0.4$ kV, and the base power, $s_{\text{base}} = 1$ kVA. All power, voltages, impedances *etc*., are transformed accordingly. The transformer voltage is $u_s = 1$ pu, from which we allow a variation of $\pm 6\%$.

In all experiments, we let

$$p_{\text{pv},h}(t) = [p_{\text{pv,base}}(t) + \mathcal{N}(0, 0.2)]_+, \quad \forall h \in H_{\text{pv}}, t \in \mathcal{T},$$

where $p_{\text{pv,base}}(t)$ is the baseline solar power presented in Fig. 5, $[\,\cdot\,]_+$ denotes positive truncation, and $\mathcal{N}(0, 0.2)$ is a zero-mean normal distribution with standard variation 0.2. We further set $s_{\text{max},h} = 6.3$ kVA, for all $h \in H_{\text{pv}}$.
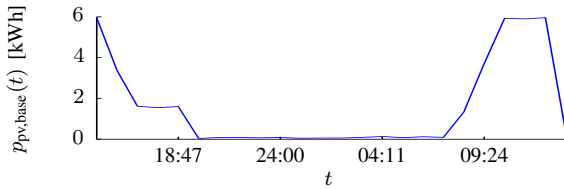

Fig. 5. The baseline solar generated power, $p_{\text{pv,base}}(t)$.

For all $h \in H_{\text{ev}}$, we let $E_{\text{dem},h} = 9$ kWh, and

$$t_{\text{ev},h} \in \mathcal{U}(2, 3), \quad E_{\text{ev},h}(t_{\text{ev},h}) \in \mathcal{U}(0, 1),$$

where $\mathcal{U}(a, b)$ denotes a uniform distribution of $[a, b]$.

A. Resilience of benchmark strategy

We evaluate the effect of installing EVs and PVs in the grid, when the benchmark strategy is utilized. The voltage profile at the connection point for each consumer in Fig. 3, is obtained by Gauss-Seidel iterations, for the following configurations:

1) $H_{\text{pv}} = \emptyset$ and $H_{\text{ev}} = \{32, 33, 34\}$;
2) $H_{\text{pv}} = \{30 - 34\}$ and $H_{\text{ev}} = \emptyset$.

The resulting voltage profiles from both configurations are presented in Fig. 6, with Configuration 1 illustrated in Fig. 6(top).
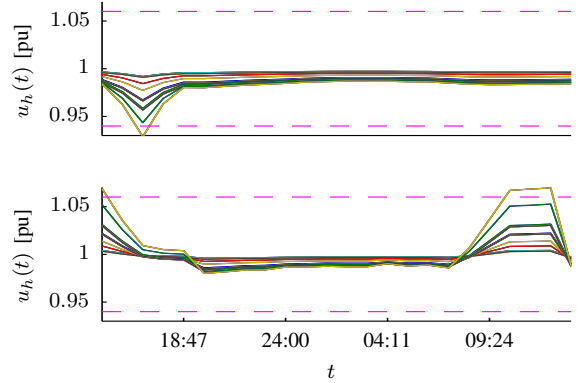

Fig. 6. Top: Voltage profile resulting each leaf by configuration 1 (solid), and allowed voltage range (dashed). Bottom: Similarly, voltage profiles by configuration 2.

Unacceptable under-voltages occur, even though only three EVs are connected. This is however associated to the specific location of the EVs in the feeder. If a similar simulation is performed with $H_{\text{ev}} = \{1, \ldots, 16\}$, the voltage deviations would be obeyed.

The converse experiment, obtained by Configuration 2 above, results in the voltage profiles presented in Fig. 6(Bottom) We see that PVs introduce local over-voltages. This is again associated to the specific location of the PVs.

B. Resilience of optimization based strategy

Employing the optimization strategy described previously, we perform again two numerical experiments, with configurations

1) $H_{\text{pv}} = \emptyset$ and $H_{\text{ev}} = H$,
2) $H_{\text{pv}} = \{30 - 34\}$ and $H_{\text{ev}} = \emptyset$.

The voltage profile obtained in the first configuration is illustrated in Fig. 7. As evident, the coordination performed by Algorithm 1, is able to support an EV for every household. It
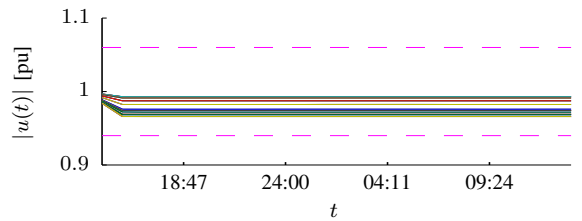

Fig. 7. Allowed voltage range (dashed), and resulting voltage profiles (solid), for the optimization based approach with $H_{\text{ev}} = H$ and $H_{\text{pv}} = \emptyset$.

is observed that all EVs are charged, roughly, with a constant power, in a way that temporally averages out the load on the grid. From further numerical studies, this result appears to be reasonably consistent, also for other configurations of H_{ev}. However, as we illustrate in the final example, this is not a valid rule-of-thumb, when $H_{\text{pv}} \neq \emptyset$.

With configuration 2 above, the optimization based approach performs no better than the benchmark strategy. This indicates that the reactive power capabilities of the PVs inverter, cannot prevent the over-voltage introduced by the local production of active power, occurring from solar panels.

C. Benefit of optimization strategy over benchmark

In this final experiment, we introduce EVs and PVs randomly throughout the feeder, such that the penetration of both PV and EV is around 50%. Employing both the benchmark and optimization based strategy, yields the results in Fig. 8, where Fig. 8(Top) and (Middle) presents the total power consumption, and the power consumption solely from EVs, respectively.

From the definition of the benchmark strategy, all EVs charge as soon as they are plugged in. This entails that there is a large peak in consumption in the beginning of the time-span of the simulation. Similarly, in the end of the simulation, when the solar power increase, there is a large negative consumption.

Conversely, when using the optimization based strategy, the EV charging is postponed, and coordinated with the PV generation, such that consumption by EVs counteracts the production from PVs.

This entails that the voltage profiles corresponding to the benchmark strategy, in Fig. 8(Bottom), initially show undervoltages when charging EVs, and later, over-voltages because the PV generated power is not absorbed. In the optimized case, however, both over- and under-voltages are avoided, by coordinating EV charge against solar power. In Fig. 8(Bottom), we see over-voltages in the very beginning of the simulation of both the benchmark and the optimized strategy. This is because at this time, there is some PV production, however, no EVs are available for charging. This illustrates an important point; that to avoid the potential over-voltages caused by PV generation, requires some flexible consumption in order to absorb the power of solar panels.

VI. Concluding remarks

In this work we have described how a future increase in the use of EVs and PVs may cause the grid to be overloaded, and unacceptable voltage variations to occur. We have arranged an optimization problem describing the issue of coordinating the flexibility posed by EVs and PV with respect to active and reactive capabilities, such that grid losses are minimized, and grid limitations are included as constraints.

Numerical experiments based on a true distribution grid located in Northern Jutland, Denmark, has illustrated how the posed optimization problem can assist in maintaining grid limitations, even when increasing the penetration of EVs and PVs far beyond the levels currently present in the Danish electric grid.

Acknowledgement

The authors wish to thank Jayakrishnan Pillai, Aalborg University, for participating in technical discussions.
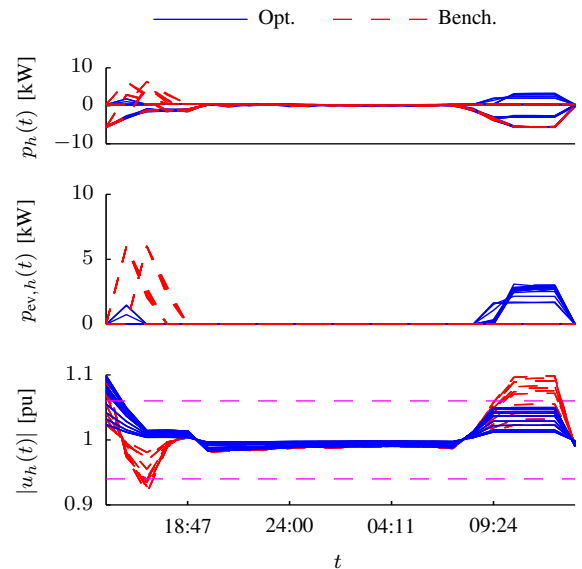

Fig. 8. Top: The total consumption in the optimized case (blue, solid), and the benchmark case (red, dashed). Middle: Corresponding EV charge schedule. Bottom: Resulting voltage profiles, as well as voltage limits (dashed, magenta).

References

[1] Danish Ministry of State, "*Et Danmark der Står Sammen*," www.stm. dk, 2011, the Danish Government Platform.
[2] Danish Energy Association and Energinet.dk, "*Smart Grid i Danmark*," www.danskenergi.dk, 2010.
[3] International Energy Agency, "*Technology Roadmap: Electric and plug-in hybrid electric vehicles*," http://www.iea.org/, 2011.
[4] J. Pillai, P. Thøgersen, J. Møller, and B. Bak, "Integration of electric vehicles in low voltage danish distribution grids," *Power and Energy*, 2012.
[5] A. Ipakchi and F. Albuyeh, "Grid of the future," *IEEE Power and Energy Magazine*, no. april, 2009.
[6] M. Juelsgaard, P. Andersen, and R. Wisniewski, "Minimization of distribution grid losses by consumption coordination," *IEEE Multi-Conference on Systems and Control*, 2013, Submitted for review.
[7] K. Turitsyn, P. Sulc, S. Backhaus, and M. Chertkov, "Options for Control of Reactive Power by Distributed Photovoltaic Generators," *Proceedings of the IEEE*, vol. 99, no. 6, pp. 1063–1073, Jun. 2011.
[8] M. E. Baran and F. F. Wu, "Network Reconfiguration in Distribution Systems for Loss Reduction and Load Balancing," *IEEE Transactions on Power Delivery*, vol. 4, no. 2, 1989.
[9] T. Hoff, "The value of grid-support photovoltaics in reducing distribution system losses," *IEEE Transactions on Energy Conversion*, vol. 10, no. 3, pp. 569–576, 1995.
[10] Y. Guo, Y. Lin, and M. Sun, "The impact of integrating distributed generations on the losses in the smart grid," *IEEE Power and Energy Society General Meeting*, 2011.
[11] P. Kundur, *Power system stability and control*. McGraw-Hill, 1993.
[12] J. Irwin and R. Nelms, *Basic Engineering Circuit Analysis*. Wiley, 2005.
[13] F. A. Viawan, "*Voltage Control and Voltage Stability of Power Distribution Systems in the Presence of Distributed Generation*," Ph.d. Thesis, 2008, chalmers University of Technology.
[14] Nord Pool Spot, http://www.nordpoolspot.com/, common Nordic Power Exchange.